

High-efficiency, energy-scalable, coherent 130-nm source by four-wave mixing in Hg vapor

C. H. Muller III, D. D. Lowenthal, and M. A. DeFaccio

Spectra Technology, Inc., 2755 Northrup Way, Bellevue, Washington, 98004

A. V. Smith

Sandia National Laboratories, Albuquerque, New Mexico, 87185

Received March 15, 1988; accepted May 24, 1988

Coherent vacuum-ultraviolet (VUV) pulses with energy of 1.1 mJ, 2.2-nsec pulse length (2 MW cm^{-2} unfocused), and measured bandwidth $\leq 0.1 \text{ cm}^{-1}$ have been achieved at 130 nm from four-wave mixing in Hg vapor. Conversion efficiencies of 5% have been demonstrated in a collimated beam geometry over 1-m interaction lengths. These high efficiencies are made possible by using two-photon-resonant sum-frequency mixing through the Hg 7^1S level. The experimental facility assembled to produce this efficient VUV source is described, and a comparison between experimental measurements and theory is provided.

Recent calculations¹⁻³ have indicated that two-photon-resonant sum-frequency mixing in Hg vapor can be an efficient (1–10%) process for the production of coherent vacuum-ultraviolet (VUV) radiation in the 120–140-nm region. In contrast to earlier experimental work, which utilizes a tightly focused geometry,⁴⁻⁶ these calculations show that efficient conversion is possible with relatively low input intensities ($5\text{--}10 \text{ MW cm}^{-2}$) and collimated nonfocused beams. The collimated geometry is important because it allows tractable modeling, area scaling of the processes to higher energies per pulse, and high optical quality of the output wave. In this Letter we report the experimental production of VUV (130-nm) light using such an approach. By using the collimated geometry we demonstrate 5% conversion efficiencies with VUV output energies of 1.1 mJ. The experimental apparatus constructed for this demonstration is described, and preliminary comparisons between experimental results and modeling predictions are presented.

A thorough discussion of efficiency-limiting mechanisms, phase-matching conditions, and input wave flux considerations for 130-nm generation is given in Ref. 3. A simplified energy-level diagram for Hg is shown in Fig. 1. One approach for 130-nm generation with collimated beams uses input frequencies $\omega_1 = 39\,212 \text{ cm}^{-1}$ (255 nm), $\omega_2 = 24\,716 \text{ cm}^{-1}$ (405 nm), and $\omega_3 = 12\,864 \text{ cm}^{-1}$ (777 nm). The 7^1S state is used for two-photon-resonant enhancement, and ω_1 and ω_2 are chosen to index match the process in pure Hg vapor for the case of parallel collimated input beams. The nonlinear susceptibility is large since, as shown in Fig. 1, the detunings from the 6^3P_1 and 8^1P_1 states are 200 and 68 cm^{-1} , respectively.

Efficient generation of 130-nm radiation in a collimated nonfocused four-wave mixing process requires single-frequency, near-diffraction-limited laser sources. Figure 2 presents a schematic of the laser

components that provide these high-quality beam lines. The fundamental wavelengths at 765, 810, and 777 nm are generated with three single-frequency ring dye-laser oscillators. These three cw beams are amplified into nanosecond pulse widths by using pulsed dye amplifiers (PDA's) pumped by frequency-doubled Nd:YAG lasers. Two stages of PDA's are used in each of the three beam lines: the first stage is a conventional three-dye-cell transversely pumped PDA; the second stage consists of a single transversely pumped dye cell. These two stages of dye amplification provide approximately 10 mJ/pulse outputs at the three fundamental wavelengths with single-mode, near-diffraction-limited beam quality.

The pump arrangement for the PDA's uses two DCR-3A Nd:YAG laser systems. The first DCR-3A is employed as a standard oscillator but is injection seeded. The seeded DCR-3A provides a temporally

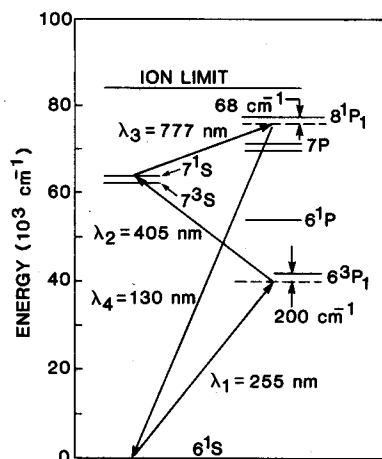


Fig. 1. Simplified energy-level diagram for Hg showing mixing scheme for the production of 130.2-nm radiation.

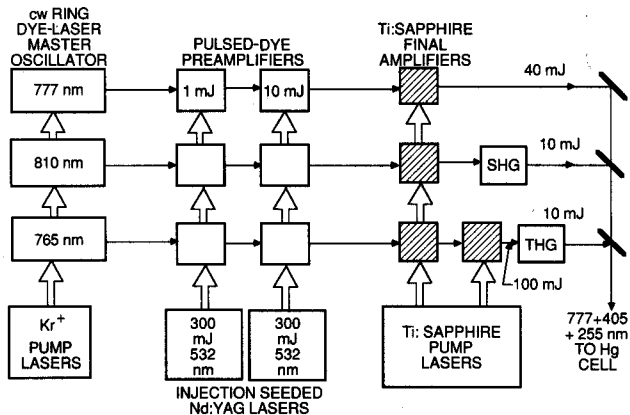


Fig. 2. Schematic of laser system components and the arrangement for producing three high-quality, single-frequency beam lines for four-wave mixing. SHG, second-harmonic generation; THG, third-harmonic generation.

smooth pulse output that is completely free of longitudinal mode beating. The frequency-doubled output from this Nd:YAG oscillator is used to pump the three first-stage PDA units. Residual $1.06\text{-}\mu\text{m}$ radiation from the first DCR-3A is then amplified in the second DCR-3A Nd:YAG system and used to pump the three second-stage PDA units. Thus, each of the six PDA's is pumped with approximately 100 mJ of single-mode 532-nm radiation.

The next stage of laser amplification is generated by Nd:YAG-pumped Ti:sapphire. An actively mode-locked Q-switched train from a commercial Quantronix Nd:YAG laser system is used to pump the Ti:sapphire. The mode-locked output train is composed of $\approx 100\text{-psec}$ pulses spaced at $\approx 10\text{-nsec}$ intervals in a total train length of $\approx 200\text{ nsec}$. This Quantronix output train is preamplified in a DCR-2A Nd:YAG laser system; the output is then split equally, and each of these beams is amplified further in two more DCR-2A Nd:YAG units. The final configuration delivers two beam lines, each with 400 mJ of frequency-doubled Nd:YAG output. The first of these two beam lines is divided equally into three parts and is used to pump three first-stage Ti:sapphire amplifiers for the 765-, 810-, and 777-nm fundamental wavelengths. This amplification stage brings each of these wavelengths up to a maximum of 40 mJ/pulse. The second mode-locked beam line is used to pump a fourth Ti:sapphire amplifier in the 765-nm beam line, bringing this energy up to 100 mJ/pulse. The 765-nm radiation is tripled (doubled and mixed) in frequency to 255 nm, while the 810-nm wavelength is doubled in frequency to 405 nm. The 255-, 405-, and 777-nm beams are combined and overlapped before reaching the Hg cell. Typical input-pulse energies to the Hg cell are 10 mJ at 255, 405, and 777 nm.

Figure 3 shows a schematic of the 1.1-m-long Hg vapor four-wave mixing cell. This Hg cell is a hot cell design in which the windows, cell body, pressure transducers, etc. are maintained at a constant temperature of 200°C . The ultrahigh-vacuum stainless-steel cell is assembled from standard Varian Conflat parts. However, the standard copper gaskets are silver plated to

prevent reaction with Hg vapor. The Hg vapor pressure is controlled with an external cold finger. The 7.62-cm (3-in.) -diameter MgF_2 input and output Brewster windows are sealed to the stainless-steel cell with a silicon-based cement.⁷ The output end of the Hg cell is interfaced to a vacuum diagnostics box that contains a LiF prism for separating the 130-nm radiation from the 777-, 405-, and 255-nm input wavelengths. Both ends of the Hg cell outside the oven are evacuated to prevent heat loss and maintain high window temperatures. The 130-nm energy, E_{130} , is measured with a Laser Precision energy monitor. This device is located in a small nitrogen-purged cavity connected to the vacuum diagnostics box. A MgF_2 window separates the two regions.

Accurate knowledge of the window and prism transmission at 130 nm is critical in determining conversion efficiency. Transmission, T , of the MgF_2 windows (250°C , $T = 46\%$; 20°C , $T = 50\%$) was measured with an oxygen discharge lamp and the input VUV spectrometer as shown in Fig. 3. Transmission through a 1-cm path in the LiF prism was estimated to be 36% based on the measured transmission through a LiF window from the same manufacturer. Absorption in the Hg cell at 130 nm by impurities such as H_2O vapor or organics was found to be less than 5%. Consequently, approximately 92% of the generated E_{130} is absorbed in the two partially transmitting MgF_2 windows and in the LiF prism before measurement. In other words, the E_{130} produced as a result of the four-wave mixing process in the Hg cell is a factor of 12.5 greater than the measured energy after transmission through two MgF_2 windows and a LiF prism.

A natural isotopic mixture of Hg was used for the results reported in this Letter, and the mass 202 two-photon-resonant 7^1S transition was excited in exact resonance. The Hg 7^1S - 6^1P isotope split was clearly discernible and similar to the plot shown in Fig. 9 in Ref. 3. Exact two-photon resonance was verified by observing the 1014-nm 7^1S - 6^1P amplified spontaneous emission signal. Experiments are under way using small detuning from the 7^1S resonance, since amplified spontaneous emission is expected to limit energy conversion efficiency³ in the exact two-photon-resonant case to approximately 10%. We have also found that E_{130} saturates with increasing Hg vapor

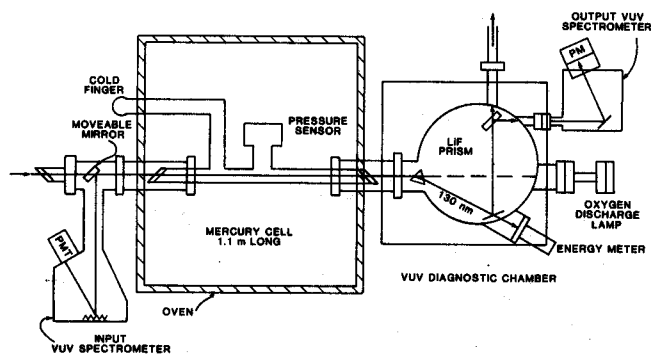


Fig. 3. Schematic of the four-wave mixing cell and VUV diagnostics. PM, PMT, photomultiplier tubes.

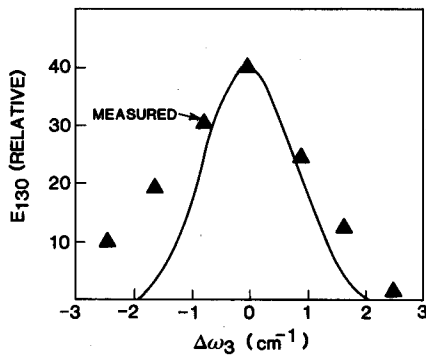


Fig. 4. Experimental (▲) versus calculated (solid line) tuning curves for the 130-nm output radiation as a function of ω_3 with ω_1 and ω_2 fixed. Note that at the peak, ω_1 , ω_2 , and $\omega_3 = 39\,212$, $24\,716$, and $12\,864\text{ cm}^{-1}$, respectively. Calculations are based on a one-dimensional model with input energies of 1.0, 1.0, and 1.2 mJ; 2.5-mm-diameter beams; and a product of Hg vapor density and mixing cell length of 10^{19} cm^{-2} .

pressure and that the optimum pressure appears to be 4–5 Torr for 1-m interaction lengths.

One-dimensional (plane-wave) and two-dimensional (Gaussian transverse profile) codes² have been written to simulate the four-wave mixing process in Hg vapor. These codes assume a temporally square pulse shape and monochromatic radiation. For laser input energies of 7.0, 8.5, and 5.5 mJ/pulse at 255-, 405-, and 777-nm wavelengths, Hg vapor pressure of 5 Torr, and 8-mm-diameter beams, the measured E_{130} is 0.083 mJ/pulse. This corresponds to approximately 1.1 mJ/pulse in the Hg cell when allowances are made for optical losses as discussed above. The energy conversion efficiency is thus 5%. This result is in excellent agreement with calculations from the two-dimensional code, which predicts a 6.2% conversion efficiency.

Sum-frequency mixing in Hg vapor is expected to be tunable between 120 and 140 nm by setting the wavelengths of the input waves for proper phase-matching conditions.² With ω_1 and ω_2 fixed, however, it is possible to obtain limited tunability by scanning ω_3 over the width of the phase-matching peak. The range of tunability depends on the product of the Hg vapor density

and the mixing cell length. For a product of 10^{19} cm^{-2} (Hg = 5 Torr and $L = 100\text{ cm}$), we calculate, using the one-dimensional codes, approximately 2-cm^{-1} tunability around 130 nm. As shown in Fig. 4, the measured tuning range is approximately 2.5 cm^{-1} under the same conditions.

In summary, we have shown that efficient two-photon-resonant sum-frequency mixing in Hg vapor is possible for the production of coherent 130-nm radiation. Collimated unfocused power densities exceeding 2 MW cm^{-2} have been produced. At present mixing efficiencies are 5%. The 130-nm radiation is tunable over 2.5 cm^{-1} with ω_1 and ω_2 fixed. Additional experiments to investigate near-resonance mixing efficiencies are under way. Experimental measurements of the beam quality and the bandwidth of the 130-nm light are also planned.

We acknowledge the contributions of J. J. Ewing and J. M. Eggleston for proposing the general experimental approach. The contribution of M. Cimolino is also gratefully acknowledged. We would also like to thank Northrop Corporation and Sandia National Laboratory for the loan of the equipment used in this experiment. This research is supported by Sandia National Laboratory under contract no. 53-8915.

References

1. A. V. Smith, G. R. Hadley, P. Esherick, and W. J. Alford, *Opt. Lett.* **12**, 708 (1987).
2. A. V. Smith and W. J. Alford, "A practical guide for 7S resonant frequency mixing in Hg: generation of light in the 230–185- and 140–120-nm ranges," *J. Opt. Soc. Am. B* (to be published).
3. A. V. Smith, W. J. Alford, and G. R. Hadley, *J. Opt. Soc. Am. B* **5**, 1503 (1988).
4. R. Mahon and F. S. Tomkins, *IEEE J. Quantum Electron.* **QE-18**, 913 (1982).
5. R. Hilbig and R. Wallenstein, *IEEE J. Quantum Electron.* **QE-19**, 1759 (1983).
6. P. R. Herman and B. P. Stoicheff, *Opt. Lett.* **10**, 502 (1985).
7. C. H. Muller III, M. W. Barrett, and D. D. Lowenthal, "High temperature window seals for VUV experiments," *Rev. Sci. Instrum.* (to be published).